# Chapter 3 Mathematical Modelling

## 3.1 Preliminary Remark

The present chapter aims to provide generalized analytical solutions for flow around single and multiple (interacting) circular/polygonal cylinders. The complex variable method is employed under the consideration of inviscid and irrotational behaviour of fluid flow known as potential flow. The mathematical description of potential flow around cylinders involves the derivation of complex potential functions and conformal maps for various configurations. It is convenient to derive complex potentials for circular domain (e.g. doublet inside circle or annulus) to obtain the analytical solution for uniform and non-uniform flows, then map these solutions around non-circular geometries (e.g. single polygonal cylinder or pair of polygonal cylinders) using conformal transformation.

The present study is based on the following assumptions:

- The fluid flow is assumed to be inviscid, irrotational, and incompressible.
- Cylinders are assumed to be placed transverse to the direction of flow.
- Fluid domain is assumed to be infinite so that the cylinders can placed at any distance from each other.
- The cylinders are assumed to be rigid having cross section uniform in spanwise direction.
- Cylinders are assumed to be of infinite length so that three-dimensional effects can be neglected and problem can be reduced to two-dimensional flow.

## 3.2 Complex Variable approach in Potential Flow

The complex variable theory is an important mathematical tool to study inviscid irrotational fluid flow, known as Potential flow. In potential flow, the flow field is described with the help of velocity potential ($\phi$) or stream function ($\psi$). The $\phi$ and $\psi$ satisfy Laplace equation ($\nabla^2\phi = 0$, $\nabla^2\psi = 0$) and in order to be holomorphic they should satisfy Cauchy- Riemann condition,

$$\frac{\partial \phi}{\partial x} = \frac{\partial \psi}{\partial y}; \; -\frac{\partial \psi}{\partial x} = \frac{\partial \phi}{\partial y}. \tag{3.1}$$

The complex potential function for two-dimensional potential flow can be mentioned by the complex combination of velocity potential ($\phi$) and stream function ($\psi$) as,

$$w\,(\zeta) = \phi(\zeta) + i\psi(\zeta), \tag{3.2}$$

where, $\zeta = x + iy$ is a complex variable.

## 3.3 Potentials Flow around Single Circular Cylinder

The uniform and non-uniform potential flow around a cylinder can be obtained by placing a point singularity (vortex or doublet) outside a cylinder at infinite and finite distance respectively. Such potential flow can be modelled using complex potential $g(\zeta)$ for irrotational free vortex (at $\zeta = \beta$) in unbounded fluid domain written as,

$$g(\zeta) = \phi + i\psi = -\frac{i}{2\pi}\log(\zeta - \beta), \tag{3.3}$$

By the application of Milne-Thomson circle theorem [26,169–171] on above function, the complex potential $w_v(\zeta, \beta)$ for the point vortex inside a unit circle can be derived,

$$w_v(\zeta, \beta) = g(\zeta) + \overline{g(\zeta)} = g(\zeta) + \overline{g(1/\bar{\zeta})}. \tag{3.4}$$

The replacement of function $g(\zeta)$ by $g(1/\bar{\zeta})$ in the conjugate part of above equation ensures that the function $w_v(\zeta, \beta)$ is analytic inside the circular domain ($|\zeta| < 1$). The function $w_v(\zeta, \delta)$ must satisfy the boundary condition such that the imaginary part of the function is constant on the boundary of cylinder,

$$Im[w_v(\zeta, \beta)] = 0, \qquad \text{on } |\zeta| = 1. \tag{3.5}$$

By substituting Equation (3.3) into Equation (3.4), the function $w_v(\zeta, \beta)$ is simplified as,

$$w_v(\zeta,\beta) = -\frac{i}{2\pi}log\left(-\frac{\beta}{|\beta|}\right) - \frac{i}{2\pi}log(\zeta) - \frac{i}{2\pi}log\left(\frac{\zeta-\beta}{|\beta|\left(\zeta-\frac{1}{\bar{\beta}}\right)}\right). \qquad (3.6)$$

The first terms in above equation is a constant, while the second term is the complex potential function for the point vortex of unit strength located at the origin inside a unit radius circle. These terms are dropped here on as during further differentiation these terms are cancelled out. Therefore, the remaining term is the complex potential function $(w_v)$ for a point vortex of unit strength at $\zeta = \beta$ in simply connected circular domain represented as,

$$w_v(\zeta,\beta) = -\frac{i}{2\pi}log\left(\frac{\zeta-\beta}{|\beta|\left(\zeta-\frac{1}{\bar{\beta}}\right)}\right). \qquad (3.7)$$

The potential flow obtained by above complex potential function in simply connected domain $D_\zeta$ inside unit circular disc can be conformaly mapped to the domain $D_z$ outside a unit circular disc by using mapping function $Z(\zeta) = 1/\zeta$ (a point $\beta \in D_\zeta$ maps to $z_\beta \in D_Z$) as shown in Figure 3.1.

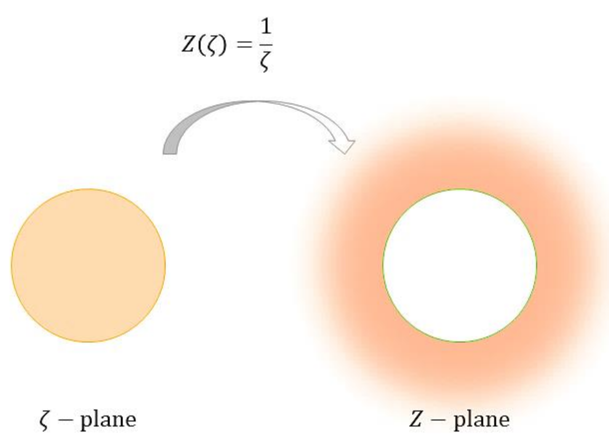


Figure 3.1 mapping from interior of circular cylinder to exterior of polygonal.

The complex potential function above provides non-uniform potential flow due to presence of stationary point vortex of unit strength outside the circular cylinder at location $z_\beta = 1/\beta$.

For the uniform potential flow parallel to $x$-axis, the complex potential function must satisfy uniform flow condition, $\mathcal{P}(Z) \to UZ$ as $Z \to \infty$ (for the vortex location $\beta \to 0$) and the boundary condition that $\Im[\mathcal{P}(Z)]$ should attain constant value on the surface of cylinder.

The uniform flow past a circular cylinder can be obtained by taking parametric derivative of complex potential function (Equation (3.7)) with respect imaginary part of vortex location $\beta = \beta_R + i\beta_I$ in complex $\zeta$-plane,

$$\mathcal{P}(\zeta, \beta) = -2\pi U \frac{\partial}{\partial \beta_I}\big(w_v(\zeta, \beta)\big). \tag{3.8}$$

By using the identities $-\frac{1}{i}\frac{\partial}{\partial \beta_I} = \frac{\partial}{\partial \bar{\beta}} - \frac{\partial}{\partial \beta}$, and substituting $w_v(\zeta, \beta)$ from Equation (3.7) in above function,

$$\mathcal{P}(\zeta, \beta) = U\left(\frac{1}{\zeta - \beta} + \frac{1}{2\beta} - \frac{1}{\bar{\beta}^2\left(\zeta - \bar{\beta}^{-1}\right)} - \frac{1}{2\bar{\beta}}\right). \tag{3.9}$$

The complex potential function in Equation (3.9) gives uniform potential flow for a doublet at location $\beta \approx 0$ ($\beta \to 0$), and non-uniform potential flow (doublet flow) around circular cylinder for $\beta \neq 0$.

The velocity ($V_c$) around a cylinder can be written as,

$$V_c = u_c - iv_c = \frac{d\mathcal{P}}{d\zeta}\Big/\frac{dZ}{d\zeta}, \tag{3.10}$$

where, $u_c$ and $v_c$ are the real and imaginary parts.

By substituting complex potential function $\mathcal{P}(\zeta, \delta)$ from Equation (3.9) and $Z = 1/\zeta$ in above equation and differentiating with respect to $\zeta$, complex velocity around circular cylinder is obtained as,

$$V_c = U\left(\frac{\zeta^2(2\beta\zeta + \zeta^2\bar{\beta}^2 - 2\zeta\bar{\beta} - \beta^2 - \zeta^2 + 1)}{\left(\zeta\bar{\beta} - 1\right)^2(\beta - \zeta)^2}\right). \tag{3.11}$$

By using Bernoulli’s theorem, the pressures distribution around the circular cylinders in potential flow can be obtained in terms of non-dimensional pressure coefficient $Cp$ as shown below,

$$Cp_c = 1 - \frac{V_c^2}{U^2} = 1 - \left(\frac{\zeta^2\left(2\beta\zeta + \zeta^2\bar{\beta}^2 - 2\zeta\bar{\beta} - \beta^2 - \zeta^2 + 1\right)}{\left(\zeta\bar{\beta} - 1\right)^2(\beta - \zeta)^2}\right)^2. \tag{3.12}$$

For $\beta = 0$ and $\zeta = 1/Z$, the above Equation (3.11) and Equation (3.12) for velocity and pressure field respectively derived using present method are converge to the relations similar to those derived using principle of superposition (Equation (A.5) and Equation (A.10) in Appendix. A) for uniform potential flow around unit circular cylinder.

## 3.4 Potential Flow around Single Polygonal Cylinder

The uniform and non-uniform potential flow around polygonal shaped cylinders with rounded corners are obtained in two steps as shown in Figure 3.2. In first step, the interior of circle ($\zeta$-plane) is mapped to the exterior of circle ($Z$-plane) using inverse map. In second step, the area around circle ($Z$-plane) is mapped to the area around polygon ($F$-plane) using hypotrochoidal map.

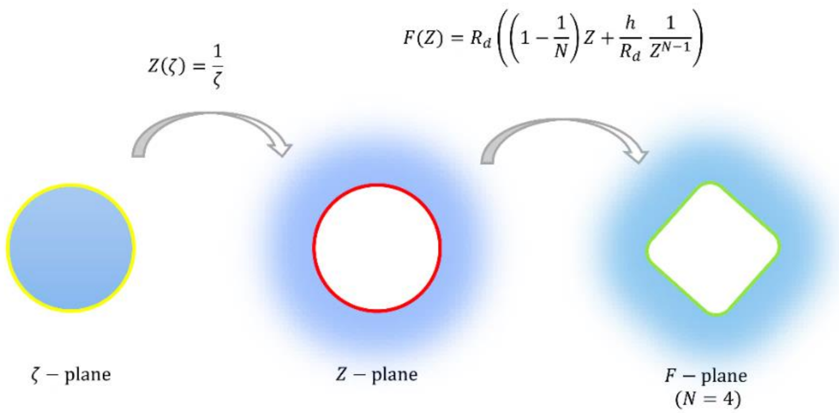


Figure 3.2 Composite mapping from interior of circular cylinder to exterior of polygonal shaped cylinder. First, interior of circle is mapped to the exterior of circle by using inverse map, further exterior of circle is mapped to polygonal shaped geometry using hypotrochoid mapping.

### *3.4.1 Hypotrochoidal Mapping*

A hypotrochoid is a locus of a point on the circular lamina (generating solid circle) rolling without sliding inside another circle (directing circle), the parametric equation of which is as follows,

$$x(\theta) = (R_d - R_r)\cos(\theta) + h\cos\left(\frac{R_d - R_r}{R_r}\theta\right);$$
$$y(\theta) = (R_d - R_r)\sin(\theta) + h\sin\left(\frac{R_d - R_r}{R_r}\theta\right). \tag{3.13}$$

where, '$R_d$' is radius of directing circle, '$R_r$' is radius of rolling circle, and '$h$' is radial distance from curve tracing point to the center of rolling circle ($0 \le h \le R_r$).

The above parametric equations of hypotrochoid in complex notation can be written like this,

$$x(\theta) + iy(\theta) = (R_d - R_r)e^{i\theta} + h\, e^{-i\left(\frac{R_d - R_r}{R_r}\theta\right)}. \tag{3.14}$$

The following mapping function ([97,98,172,173]) is developed using above parametric equations of hypotrochoid,

$$F = f(Z) = R_d\left(\left(1 - \frac{1}{N}\right)Z + \frac{h}{R_d}\,\frac{1}{Z^{N-1}}\right), \tag{3.15}$$

where, '$N$' is the ratio of radius of directing circle ($R_d$) to the radius of generating circle ($R_r$). In order to have a closed curve, the ratio $'N'$ should integer ($N \ge 2$). The corner radius and straightness of the sides of polygonal depend on the value of '$h$' ( $0 \le h \le R_r$).

In mapping function shown in Equation (3.15), for $h = 0$, ($\forall N \ge 2$) and for $h = R_r$, $N \ge 2$, circle and hypocycloids with '$N$' sides can be traced. Other values of '$h$' ($0 < h < R_r$) generates polygonal shapes with finite corner radius (refer Figure 3.3).

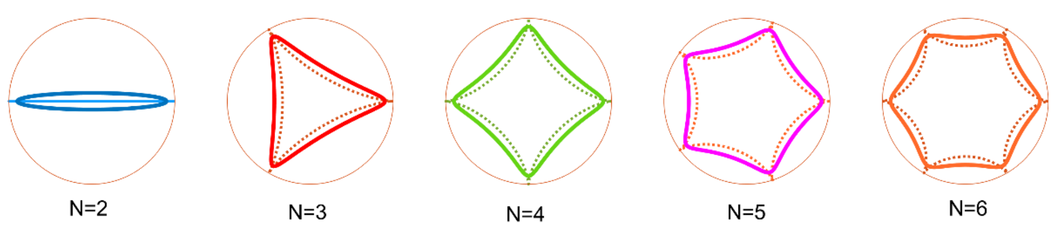


Figure 3.3 Various polygonal shapes obtained using hypotrochoidal mapping Function. Continues lines shows hypocycloid with cusps drawn when ($h = R_r$), and dotted lines shows hypotrochoid drawn with finite corner radius when ($0 < h < R_r$).

### *3.4.2 Velocity and Pressure Field*

The velocity around polygonal shaped cylinders is obtained using complex potential function $\mathcal{P}(\zeta, \delta)$ in combination with hypotrochoidal mapping (Equation (3.15)) as shown below,

$$V = R_d \left(1 - \frac{1}{N}\right)\left(\frac{d\mathcal{P}}{d\zeta} \Big/ \frac{dF}{d\zeta}\right). \tag{3.16}$$

In hypotrochoidal mapping (Equation (3.15)), for $h \to 0$, function takes the form $F \approx R_d(1 - 1/N)Z$, which maps a circular geometry to the $F$-complex plane of reduced size by an amount of $R_d(1 - 1/N)$, also it tends to increase velocity around a circular cylinder by $1/[R_d(1 - 1/N)]$ times. In order to avoid this problem of dependency of velocity on size of cylinder in the unbounded fluid region, the differentiation term in Equation (3.16) is multiplied by $R_d(1 - 1/N)$. By performing the differentiation, the velocity around the polygonal shaped cylinders rotated by an angle '$\gamma$' is expressed as,

$$V = \frac{-R_d\, |V_c|\, (e^{i\gamma})^N}{-R_d\, (e^{i\gamma})^N + h\, N\, \zeta^N}. \tag{3.17}$$

Above equation of complex velocity ($V$) can be simplified to find velocity profile ($V^s$) on the surface of polygonal shaped cylinders,

$$V^s = \frac{2R_d\, U\, (e^{i\gamma})^N\, |\sin(\theta)|}{-R_d\, (e^{i\gamma})^N + h\, N\, \zeta^N}. \tag{3.18}$$

In the above equation, the condition for infinite velocity ($V^s \to \infty$) on the surface can be obtained by taking,

$$-R_d\, (e^{i\gamma})^N + h\, N\, \zeta^N = 0. \tag{3.19}$$

By substituting $hN = R_d$ for $h = R_r$ in above equation, we get,

$$\zeta^N = \left(e^{i\gamma}\right)^N. \tag{3.20}$$

By comparing real and imaginary parts, we get,

$$\theta_n = \gamma + \frac{(n-1)2\pi}{N}, \tag{3.21}$$

where, $n = 1, \dots, N$. Angle $\theta_n$ in above equation gives location of points on the surface of polygonal shaped cylinders, where velocity becomes infinity. These points are the cusp points of hypocycloid.

The equation of pressure co-efficient $Cp$ around polygonal shaped cylinders can be written as follows using Bernoulli's principle (Equation A.9 in Appendix-A),

$$Cp = 1 - \left( \frac{R_d \; V_c (e^{i\gamma})^N}{U \; (-R_d \; (e^{i\gamma})^N + \; h \, N \; \zeta^N)} \right)^2 . \tag{3.22}$$

The pressure co-efficient on the surface of polygonal shaped cylinder can be represented as,

$$Cp^s = 1 - \left( \frac{2|\sin(\theta)| \; R_d \; (e^{i\gamma})^N}{-R_d \; (e^{i\gamma})^N + \; h \, N \; \zeta^N} \right)^2 . \tag{3.23}$$

The surface pressure co-efficient $Cp^s$ on polygonal shaped cylinder becomes equal to that on the surface of circular cylinder (Equation (3.12)) for $h = 0$.

## 3.5 Potential Flow around Two Circular Cylinders

The uniform potential flow around two circular cylinders is investigated by computing the complex potential function for a doublet inside an annulus and mapping it to the infinite location outside the pair of non-overlapping circles using bilinear mapping.

### *3.5.1 Bilinear Mapping*

In order to investigate the hydrodynamic interaction between two circular cylinders, the concentric annular area between two circles $q \leq |\zeta| \leq 1$ in $\zeta$-plane is conformally mapped to the area outside circles $C_1{}'(|\xi| = 1)$ and $C_2'(|\xi - H| = R_1)$ in physical $\xi$-plane as shown in Figure 3.4 by using following bilinear conformal mapping,

$$\xi_j = \frac{\zeta_j - \lambda}{\zeta_j \lambda - 1}, \tag{3.24}$$

where, $\zeta_j$ is written as $\zeta_1 = e^{i\theta}$ for $j = 1$ and $\zeta_2 = q e^{i\theta}$ for $j = 2$.

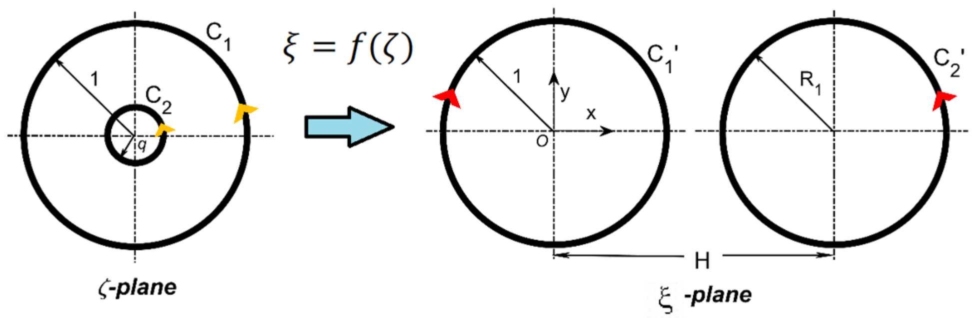


Figure 3.4 Doubly connected geometries (a) Annulus formed by circle of radius 1 and $q$ in $\zeta$-plane (b) Two circular cylinder in $\xi$-plane obtained from annulus through bilinear mapping.

The real constant $\lambda$ and the radius $q$ of circle $C_2$ are determine by mapping points on the real axis in $\zeta$-plane to the points on real axis in $\xi$-plane (Appendix-B) as given below,

$$\lambda = \frac{1}{2H}\left(H^2 + 1 - R_1^2 + \sqrt{(H^2 - (1 + R_1)^2)(H^2 - (1 - R_1)^2)}\right), \tag{3.25}$$

and,

$$q = \frac{R_1 + H - \lambda}{\lambda(R_1 + H) - 1}, \tag{3.26}$$

The cylinders in $\xi$-plane follows non-overlapping condition,

$$H > 1 + R_1. \tag{3.27}$$

### *3.5.2 Complex Potential Function*

The complex potential function for a singularity (vortex) trapped at $\zeta = \beta$ in an annulus domain formed between two concentric circles $\zeta_1 = e^{i\theta}$ and $\zeta_2 = qe^{i\theta}$ is presented as ([169,170]),

$$W_v(\zeta, \beta) = -\frac{i}{2\pi} log\left(\frac{|\beta| P(\zeta\beta^{-1}, q)}{P(\zeta\bar{\beta}, q)}\right), \tag{3.28}$$

where, the $P$-function can be written in form of Laurent series expansion as shown below,

$$P(\zeta\beta^{-1}, q) = A \sum_{n=-\infty}^{\infty} (-1)^n \, q^{n(n-1)} \, (\zeta\beta^{-1})^n ; \tag{3.29}$$

$$P(\zeta\bar{\beta}, q) = A \sum_{n=-\infty}^{\infty} (-1)^n \, q^{n(n-1)} \, (\zeta\bar{\beta})^n,$$

where,

$$A = \prod_{n=1}^{\infty} (1 + q^{2n})^2 \Bigg/ \sum_{n=0}^{\infty} q^{n(n-1)}. \tag{3.30}$$

By differentiating the function $W_v(\zeta, \beta)$ (Equation (3.28)) with respect to $\beta$ and $\bar{\beta}$, the complex potential function for doublet at $\zeta = \beta$ in $\zeta$-plane (inside an annulus) corresponds to the uniform potential flow in $\xi$-plane (outside two circles) can be written as,

$$W_U(\zeta_j, \beta) = 2\pi U a i \left[ e^{-i\alpha} \frac{\partial}{\partial \bar{\beta}} - e^{i\alpha} \frac{\partial}{\partial \beta} \right] W_v(\zeta_j, \beta), \tag{3.31}$$

where, '$\alpha$' is flow angle and '$a$' is a real constant associated with conformal mapping.

For uniform potential flow around two circular cylinders, the constant '$a$' in above function can be obtained by rewriting bilinear mapping function as,

$$\xi_j = \frac{(\zeta_j/\lambda) - 1}{\zeta_j - 1/\lambda}, \tag{3.32}$$

By evaluating the mapping function (Equation (3.32)) at pole $\zeta_j = 1/\lambda$, the constant '$a$' is determined as,

$$a = \frac{1}{\lambda^2} - 1\,. \tag{3.33}$$

After substituting complex potential function $W_v$ (Equation (3.28)) for point vortex in an annulus and constant '$a$' (Equation (3.33)) in Equation (3.31),

$$W_U(\zeta_j, \beta) = \left(\frac{1}{\lambda^2} - 1\right) \frac{U}{\beta} \left[ i \, sin\alpha + \left( e^{-i\alpha} \, \frac{\zeta\beta^{-1} P_\zeta(\zeta\beta^{-1}, q)}{P(\zeta\beta^{-1}, q)} - e^{i\alpha} \, \frac{\zeta\beta P_\zeta(\zeta\beta, q)}{P(\zeta\beta, q)} \right) \right], \tag{3.34}$$

where, $P_\zeta(\zeta\beta, q)$ and $P_\zeta(\zeta\beta^{-1}, q)$ are the differentiation of $P$-function with respect to the first argument of function,

$$P_\zeta(\zeta\beta, q) = A \sum_{n=-\infty}^{\infty} (-1)^n \, q^{n(n-1)} \, n(\zeta)^{n-1}\,;$$
$$P_\zeta(\zeta\beta^{-1}, q) = A \sum_{n=-\infty}^{\infty} (-1)^n \, q^{n(n-1)} \, n(\zeta\beta^{-1})^{n-1}. \tag{3.35}$$

In above formulation of complex potential function, the value of $\beta = 1/\lambda$ maps uniform potential flow around the circular cylinder pair in $\xi$-plane.

### *3.5.3 Velocity and Pressure Field*

The velocity and pressure field around the pair of circular cylinders in $\xi$-plane is obtained by taking differentiation of complex potential function $W_U(\zeta, \beta)$ (Equation (3.34)) and bilinear mapping function (Equation (3.24)) as written below,

$$V_j = -\frac{U}{\beta}\left(\frac{\left(\zeta_j\lambda - 1\right)^2}{\lambda^2}\right)\left[\begin{pmatrix} \mathrm{e}^{-i\alpha}\left\{T_1\left(\zeta_j\beta^{-1}, q\right) - T_2\left(\zeta_j\beta^{-1}, q\right)\right\} \\ -\mathrm{e}^{i\alpha}\left\{T_1\left(\zeta_j\beta, q\right) - T_2\left(\zeta_j\beta, q\right)\right\} \end{pmatrix}\right], \tag{3.36}$$

and,

$$Cp_j = 1 + \frac{1}{\beta^2}\left(\frac{\left(\zeta_j\lambda - 1\right)^4}{\lambda^4}\right)\left[\begin{pmatrix} \mathrm{e}^{-i\alpha}\left\{T_1\left(\zeta_j\beta^{-1}, q\right) - T_2\left(\zeta_j\beta^{-1}, q\right)\right\} \\ -\mathrm{e}^{i\alpha}\left\{T_1\left(\zeta_j\beta, q\right) - T_2\left(\zeta_j\beta, q\right)\right\} \end{pmatrix}\right]^2, \tag{3.37}$$

where,

$$T_1(\zeta\beta^{-1}, q) = \frac{\zeta_j\beta^{-2}P_{\zeta\zeta}\left(\zeta_j\beta^{-1}, q\right) + \beta^{-1}P_\zeta\left(\zeta_j\beta^{-1}, q\right)}{P\left(\zeta_j\beta^{-1}, q\right)};$$

$$T_2(\zeta\beta^{-1}, q) = \frac{\zeta_j\beta^{-2}P_\zeta^2\left(\zeta_j\beta^{-1}, q\right)}{P^2\left(\zeta_j\beta^{-1}, q\right)};$$

$$T_1(\zeta\beta, q) = \frac{\zeta_j\beta^2 P_{\zeta\zeta}\left(\zeta_j\beta, q\right) + \beta P_\zeta\left(\zeta_j\beta, q\right)}{P\left(\zeta_j\beta, q\right)};$$

$$T_2(\zeta\beta, q) = \frac{\zeta_j\beta^2 P_\zeta^2\left(\zeta_j\beta, q\right)}{P^2\left(\zeta_j\beta, q\right)}.$$

In above equations, the terms $P_\zeta$ and $P_{\zeta\zeta}$ represents first order and second order differentiation of $P$-function respectively with respect to the first argument of function.

### *3.5.4 Hydrodynamic Forces*

The complex hydrodynamic force $F_{x_j} - iF_{y_j}$ acting on $j^{\text{th}}$ circular cylinder during the hydrodynamic interaction in the fluid of density $\varrho$ is obtained by using Blasius integral theorem, as shown in below equation,

$$F_{x_j} - iF_{y_j} = \frac{i\varrho}{2}\oint\left(\frac{dW_U}{d\xi}\right)^2 d\xi, \tag{3.38}$$

where, $F_{x_j}$ is the force component along the $x$-axis direction and $F_{y_j}$ is the force component along the $y$-axis direction acting on $j^{\text{th}}$ circular cylinder.

By performing change of variable,

$$F_{x_j} - iF_{y_j} = \mp\frac{i\rho}{2}\oint\left(\frac{dW_U}{d\zeta}\right)^2\left(\frac{d\zeta}{d\xi}\right)^{-1} d\zeta, \tag{3.39}$$

where, change of variable in the integrand changes the direction of the integration.

After substituting differentiation of complex potential function (Equation (3.34) and bilinear mapping function (Equation (3.24)),

$$F_{x_j} - iF_{y_j} = \mp\frac{i\varrho}{2}\frac{U}{\beta\lambda^2}\oint\left(\zeta_j\lambda - 1\right)^2\begin{pmatrix}\mathrm{e}^{-i\alpha}\left\{T_1\left(\zeta_j\beta^{-1}, q\right) - T_2\left(\zeta_j\beta^{-1}, q\right)\right\} \\ -\mathrm{e}^{i\alpha}\left\{T_1\left(\zeta_j\beta, q\right) - T_2\left(\zeta_j\beta, q\right)\right\}\end{pmatrix}^2 d\zeta \tag{3.40}$$

The forces in above equation can also be represented in terms of non-dimensional force co-efficient $C_{fx_j}$ and $C_{fy_j}$ as shown below,

$$C_{f_{x_j}} - iC_{f_{y_j}} = \frac{F_{x_j} - iF_{y_j}}{\frac{1}{2}\varrho U^2 D_j}, \tag{3.41}$$

where, $D_j$ is the diameter of $j^{th}$ cylinder.

## 3.6 Potential Flow around Pair of Polygonal and Circular Cylinders

The uniform potential flow around the pair of polygonal and circular cylinder is obtained using composition of bilinear and hypotrochoidal mapping along with complex potential for doublet inside an annulus.

### *3.6.1 Mapping from Annulus to Polygonal-Circular Geometry*

In doubly connected domain, polygonal cylinder ($C_1$) with rounded corners centred at the origin and circular cylinder ($C_2$) located at distance $H$ away from origin in the physical $Z$-plane is considered as shown in Figure 3.5. To obtain this polygonal-circular geometry, the annular area between two circles in $\zeta$-plane is first mapped to the area outside two unit-radius circles in $\xi$-plane using bilinear mapping, then the area outside two circles is mapped to the area outside the polygonal-circular geometry in $Z$-plane using hypotrochoidal mapping.

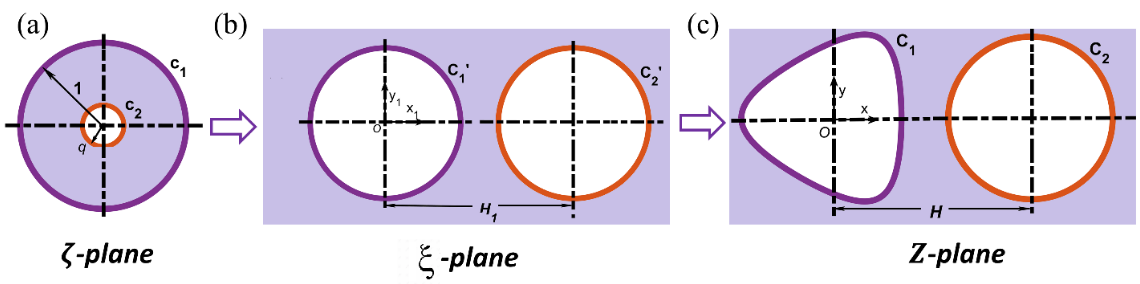


Figure 3.5 Geometries in doubly connected case (a) Annulus formed between the circles of unit radius and radius $q$ in $\zeta$-plane (b) pair of unit-radius circles in $\xi$-plane mapped from the annulus in $\zeta$-plane using bilinear mapping (c) pair of rounded corners polygonal ($N = 3$) and unit radius circular geometry in $Z$-plane mapped from pair of circles in $\xi$-plane using hypotrochoidal mapping.

The bilinear mapping function in Equation (3.24) conformally maps the annulus $q \leq |\zeta| \leq 1$ (the outer circle $c_1$of unit radius and inner circle $c_2$ of radius $q$) from $\zeta$-plane to infinite region with two non-overlapping circles $C_1{}'$ ($|\xi_1| = 1$) and $C_2{}'$ ($|\xi_2 - H_1| = 1$), each of unit radius at distance $H_1$ apart in $\xi$-plane.

For both circles of unit radius in $\xi$-plane, the constant $\lambda$ and radius $q$ in terms of $H_1$ are presented as,

$$\lambda = \frac{1}{2}\left(H_1 + \sqrt{(H_1^2 - 4)}\right); \qquad H_1 > 2, \tag{3.42}$$

and,

$$q = \frac{1 + H_1 - \lambda}{\lambda(1 + H_1) - 1}. \tag{3.43}$$

The area outside two circles in $\xi$-plane is then mapped to the area outside the pair of polygonal and circular geometry in $Z$-plane by incorporating hypotrochoidal mapping (Equation (3.15)) in bilinear mapping (Equation (3.24)),

$$Z_j(\zeta_j) = \left(1 - \frac{1}{N}\right)\left(\frac{\zeta_j - \lambda}{\zeta_j\lambda - 1}\right) + h\left(\frac{\zeta_j - \lambda}{\zeta_j\lambda - 1}\right)^{1-N} exp\,(i\gamma N), \tag{3.44}$$

where, '$\gamma$' is an angle by which polygon is rotated from positive real axis in $Z$-plane. The polygon thus obtained is inscribed in a circle with radius $(1 - (1/N) + h)$.

For flow around pair of polygonal-circular cylinder, the constant '$a$' in the Equation (3.31) can be determined by rewriting the above mapping function in the following form,

$$Z_j(\zeta_j) = \frac{a}{\zeta_j - 1/\lambda} + h\left[\frac{a}{\left(\zeta_j - \frac{1}{\lambda}\right)\left(1 - \frac{1}{N}\right)}\right]^{1-N} ex\,p(i\gamma N). \tag{3.45}$$

By evaluating the mapping function at pole $\zeta_j = 1/\lambda$, the constant '$a$' can be determined as,

$$a = \left(1 - \frac{1}{N}\right)\left(\frac{1}{\lambda^2} - 1\right). \tag{3.46}$$

### *3.6.2 Complex Potential Function*

The complex potential function for doublet flow in an annulus ($\zeta$-plane) that corresponds to the flow around polygonal-circular cylinders ($Z$-plane) is obtained by substituting complex potential function $W_v$ (Equation (3.28)) and constant '$a$' (Equation (3.46)) into Equation (3.31) as follows,

$$W_U(\zeta,\beta) = \frac{U}{\beta}\left(1-\frac{1}{N}\right)\left(\frac{1}{\lambda^2}-1\right)\left(i\sin(\alpha) + \begin{pmatrix} e^{-i\alpha}\ \dfrac{\zeta\beta^{-1}P_\zeta(\zeta\beta^{-1},q)}{P(\zeta\beta^{-1},q)} \\ -e^{i\alpha}\ \dfrac{\zeta\beta P_\zeta(\zeta\beta,q)}{P(\zeta\beta,q)} \end{pmatrix}\right). \qquad (3.47)$$

### *3.6.3 Velocity and Pressure around the Cylinders*

The complex potential function given by Equation (3.47) and composite mapping function given by Equation (3.44) are now differentiated with respect to $\zeta$ to obtain velocity field $V_j$ and pressure co-efficient $Cp_j$ around polygonal-circular cylinder pair as written below,

$$V_j = \frac{U}{S_j\beta}\left(\mathrm{e}^{-i\alpha}\{T_1(\zeta_j\beta^{-1},q) - T_2(\zeta_j\beta^{-1},q)\} - \mathrm{e}^{i\alpha}\{T_1(\zeta_j\beta,q) - T_2(\zeta_j\beta,q)\}\right), \qquad (3.48)$$

and,

$$Cp_j = 1 - \frac{1}{S_j^2\beta^2}\begin{pmatrix} \mathrm{e}^{-i\alpha}\{T_1(\zeta_j\beta^{-1},q) - T_2(\zeta_j\beta^{-1},q)\} \\ -\mathrm{e}^{i\alpha}\{T_1(\zeta_j\beta,q) - T_2(\zeta_j\beta,q)\} \end{pmatrix}^2, \qquad (3.49)$$

where, the terms $T_1(\zeta\beta^{-1},q), T_2(\zeta\beta^{-1},q), T_1(\zeta\beta,q)$, and $T_2(\zeta\beta,q)$ are already defined in Section (3.5.3) and,

$$S_j = \left(\frac{-\lambda^2(\zeta_j\lambda-1)^{N-2}}{(\zeta_j-\lambda)^N}\right)\left\{\left(\frac{\zeta_j-\lambda}{\zeta_j\lambda-1}\right)^N - hN\exp\,(i\gamma N)\right\}.$$

The above relations for velocity (Equation (3.48)) and pressure (Equation (3.49)) around the pair of polygonal-circular cylinders can be converted to Equation (3.36) and Equation (3.37) respectively for the hydrodynamic interaction between two equal circular cylinders for $h = 0$.

### *3.6.4 Hydrodynamic Forces*

The hydrodynamic forces $F_{x_j} - iF_{y_j}$ acting on $j^{\text{th}}$ cylinder by the fluid of density $\varrho$ can be obtained by integrating pressure field on the cylinder boundary $C_j$ using Blasius theorem as shown below,

$$F_{x_j} - iF_{y_j} = \mp \frac{i\varrho}{2} \oint \left(\frac{dW_U}{d\zeta_j}\right)^2 \left(\frac{dZ_j}{d\zeta_j}\right)^{-1} d\zeta_j. \tag{3.50}$$

By substituting differentiation of complex potential (Equation (3.47)) and composite conformal map (Equation (3.44)) in above relation, the force acting on cylinders can be written as,

$$F_{x_j} - iF_{y_j} = \mp \frac{i\varrho U^2}{2\beta^2}\left(1 - \frac{1}{N}\right)\left(\frac{1}{\lambda^2} - 1\right) \oint \frac{1}{S_j} \begin{pmatrix} \mathrm{e}^{-i\alpha}\{T_1(\zeta_j\beta^{-1}, q) - T_2(\zeta_j\beta^{-1}, q)\} \\ -\mathrm{e}^{i\alpha}\{T_1(\zeta_j\beta, q) - T_2(\zeta_j\beta, q)\} \end{pmatrix}^2 d\zeta_j. \tag{3.51}$$

The forces in above equation can also be represented in terms of non-dimensional force co-efficient $C_{fx_j}$ and $C_{fy_j}$ as shown in Equation (3.41).

## 3.7 Flow around Polygonal-Polygonal Cylinder Pair

In this section, the mathematical formulation for the uniform potential flow of free stream velocity $U$ at flow angle $\alpha$ around the pair of polygonal cylinders separated by center distance $H$ in physical $Z$-plane is carried out.

### *3.7.1 Mapping from Annulus to Polygonal-Polygonal Geometry*

Consider two polygonal cylinders $Z_1$ and $Z_2$ with number of sides $N_1$ and $N_2$, and corner radii $\rho_1$ and $\rho_2$ respectively. The Cylinder-1 ($Z_1$) is located at origin of the reference frame, while the Cylinder-2 ($Z_2$) is placed $H$ distance away from the origin in the physical $Z$-plane. The pair of polygonal-polygonal geometry in $Z$-plane is conformally mapped from the annulus in $\zeta$-plane in two stages as shown in Figure 3.6.

In first stage, the concentric annulus $q \leq |\zeta| \leq 1$ in $\zeta$-plane is mapped onto infinite region around two non-overlapping unit-radius circles separated by center-to-center distance $H$ using bilinear map (Equation (3.24)). In second stage, two unit-circles in $\xi$-plane are mapped to the two-polygons in $Z$-plane by the application of hypotrochoidal transformation (Equation (3.15)).

The bilinear and hypotrochoidal mapping functions are combined to get a composite map as follows,

$$Z_j(\zeta_j) = \left[\left(1-\frac{1}{N_j}\right)\left\{\left(\frac{\zeta_j-\lambda}{\zeta_j\lambda-1}\right)-\mathcal{C}_j\right\}+h_j\left\{\left(\frac{\zeta_j-\lambda}{\zeta_j\lambda-1}\right)-\mathcal{C}_j\right\}^{1-N_j}\exp(-i\gamma_j N_j)\right] + \mathcal{C}_j, \tag{3.52}$$

where, $N_j$ is the number of sides, $h_j$ is a distance of curve tracing point from center of rolling circle, $\gamma_j$ is the angle of orientation (measured from positive real axis) and $\mathcal{C}_j$ is the distance from the origin ($\mathcal{C}_1 = 0$ and $\mathcal{C}_2 = H$) of $j^{th}$ polygonal geometry in $Z$-plane.

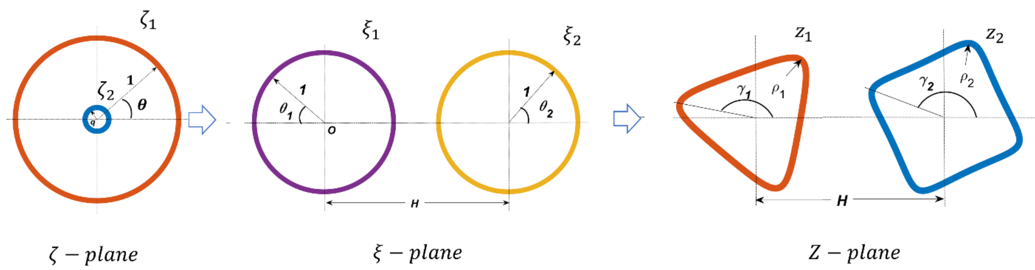


Figure 3.6 Conformal mapping from annulus formed between two concentric circles of unit radius and radius $q$ in $\zeta$-plane to the pair of two unit-radius circles at distance $H$ in $\xi$-plane using bilinear mapping and further mapping to the cylinder pair of polygonal sections of different number of sides ($N_j$), corner radius ($\rho_j$), and orientation angle ($\gamma_j$) in $Z$-plane using hypotrochoidal mapping.

By evaluating above mapping function at pole $\zeta = 1/\lambda$, the constant $a_j$ in Equation (3.31) is determined as,

$$a_j = \left(1-\frac{1}{N_j}\right)\left(\frac{1}{\lambda^2}-1\right). \tag{3.53}$$

### *3.7.2 Complex Potential Function*

Following complex potential function is obtained for uniform potential flow around two polygonal cylinders in $Z$-plane by substituting $W_v(\zeta,\delta)$ from Equation (3.28) and constant '$a_j$' from Equation (3.53) into Equation (3.31),

$$W_U(\zeta,\beta) = \frac{U}{\beta}\left(1-\frac{1}{N_j}\right)\left(\frac{1}{\lambda^2}-1\right)\left(e^{-i\alpha}\frac{\zeta\,\beta^{-1}P_\zeta(\zeta\beta^{-1},q)}{P(\zeta\beta^{-1},q)} - e^{i\alpha}\frac{\zeta\beta P_\zeta(\zeta\beta,q)}{P(\zeta\beta,q)}\right), \tag{3.54}$$

where, $P_\zeta(\zeta\beta^{-1},q)$ and $P_\zeta(\zeta\beta,q)$ are the differentiation of $P$-function (Equation (3.35)).

### *3.7.3 Velocity around Cylinders*

By differentiating composite mapping (Equation (3.52)) and complex potential $W_U(\zeta,\beta)$ (Equation (3.54)), the equation for velocity and pressure distribution on the surface of $j^{th}$ polygonal cylinder can be written as,

$$V_j = \frac{U}{\mathcal{S}_j\beta}\begin{bmatrix} \mathrm{e}^{-i\alpha}\left(\beta^{-1}\mathcal{T}(\zeta_j\beta^{-1},q) + \frac{1}{\zeta_j}\mathcal{F}(\zeta_j\beta^{-1},q)\{1-\mathcal{F}(\zeta_j\beta^{-1},q)\}\right) \\ -\mathrm{e}^{i\alpha}\left(\beta\mathcal{T}(\zeta_j\beta,q) + \frac{1}{\zeta_j}\mathcal{F}(\zeta_j\beta,q)\{1-\mathcal{F}(\zeta_j\beta,q)\}\right) \end{bmatrix}, \tag{3.55}$$

and,

$$Cp_j = 1 - \frac{1}{{\mathcal{S}_j}^2\beta^2}\Bigg[\mathrm{e}^{-i\alpha}\left(\beta^{-1}\mathcal{T}(\zeta_j\beta^{-1},q) + \frac{1}{\zeta_j}\mathcal{F}(\zeta_j\beta^{-1},q)\{1-\mathcal{F}(\zeta_j\beta^{-1},q)\}\right) \\ - \mathrm{e}^{i\alpha}\left(\beta\mathcal{T}(\zeta_j\beta,q) + \frac{1}{\zeta_j}\mathcal{F}(\zeta_j\beta,q)\{1-\mathcal{F}(\zeta_j\beta,q)\}\right)\Bigg]^2. \tag{3.56}$$

where,

$$\mathcal{T}(\zeta_j\beta^{-1},q) = \frac{\zeta_j\beta^{-1}P_{\zeta\zeta}(\zeta_j\beta^{-1},q)}{P(\zeta_j\beta^{-1},q)};\ \mathcal{F}(\zeta_j\beta^{-1},q) = \frac{\zeta_j\beta^{-1}P_{\zeta}(\zeta_j\beta^{-1},q)}{P(\zeta_j\beta^{-1},q)};$$

$$\mathcal{T}(\zeta_j\beta,q) = \frac{\zeta_j\beta P_{\zeta\zeta}(\zeta_j\beta,q)}{P(\zeta_j\beta,q)};\ \mathcal{F}(\zeta_j\beta,q) = \frac{\zeta_j\beta P_{\zeta}(\zeta_j\beta,q)}{P(\zeta_j\beta,q)};$$

and,

$$\mathcal{S}_j = \frac{-\lambda^2}{(\zeta_j\lambda-1)^2}\left[1 - h_j\, N_j e^{i\gamma_j N_j}\left(\frac{\zeta_j-\lambda}{\zeta_j\lambda-1} - \mathcal{C}_j\right)^{-N_j}\right].$$

The generalized mathematical relations are obtained above for velocity (Equation (3.55)) and pressure (Equation (3.56)) around two interacting polygonal cylinders. These relations can be converted to the relations for the hydrodynamic interaction between polygonal-circular cylinders (Equation (3.48) and Equation (3.49) respectively) and for the hydrodynamic interaction between two circular cylinders (Equation (3.36) and Equation (3.37) respectively) by substituting $h_j = 0$.

### 3.7.4 Hydrodynamic Forces

Using Blasius theorem (Equation (3.38)), the hydrodynamic forces acting on two interacting polygonal cylinders can be determined as,

$$F_{x_j} - iF_{y_j} = \mp \frac{i\varrho}{2} \oint \left( \frac{dW_U(\zeta_j, \beta)}{d\zeta_j} \right)^2 \left( \frac{dZ_j}{d\zeta_j} \right)^{-1} d\zeta_j. \tag{3.57}$$

Substituting the function $W_U(\zeta_j, \beta)$ from Equation (3.54) and conformal mapping $Z_j(\zeta)$ from Equation (3.52) in above equation, the hydrodynamic forces acting on $j^{th}$ polygonal cylinder can be written as,

$$F_{x_j} - iF_{y_j} = \mp \frac{i\varrho U^2}{2\beta^2} \left(1 - \frac{1}{N_j}\right) \left(\frac{1}{\lambda^2} - 1\right) \oint \frac{1}{\mathcal{S}_j} \begin{pmatrix} \mathrm{e}^{-i\alpha} \begin{pmatrix} \beta^{-1} \mathcal{T}(\zeta_j \beta^{-1}, q) + \\ \frac{1}{\zeta_j} \mathcal{F}(\zeta_j \beta^{-1}, q) \\ \{1 - \mathcal{F}(\zeta_j \beta^{-1}, q)\} \end{pmatrix} \\ -\mathrm{e}^{i\alpha} \begin{pmatrix} \beta \mathcal{T}(\zeta_j \beta, q) + \\ \frac{1}{\zeta_j} \mathcal{F}(\zeta_j \beta, q) \\ \{1 - \mathcal{F}(\zeta_j \beta, q)\} \end{pmatrix} \end{pmatrix}^2 d\zeta_j. \tag{3.58}$$

## 3.8 Closing Remark

In this chapter, the mathematical formulation of potential flow around single and multiple cylinders is presented using complex variable methods. The complex potentials are derived for the vortex flow, doublet flow and uniform potential flow around single circular cylinder, single polygonal cylinder, pair of circular cylinders, pair of polygonal-circular cylinders, and pair of two-polygonal cylinders. Hypotrochoidal mapping is presented to obtain $N$-sided polygonal geometries with rounded corners. For two-cylinder problem, the pair of polygonal-circular and polygonal-polygonal geometry are obtained by composition of bilinear and hypotrochoidal mapping. The equations for the velocity, pressure and hydrodynamic forces are derived for different geometrical conditions.